sustainability

MDPI

Article

An Evaluation of Dryland Ulluco Cultivation Yields in the Face of Climate Change Scenarios in the Central Andes of Peru by Using the AquaCrop Model

Ricardo Flores-Marquez [1,*], Jesús Vera-Vílchez [2], Patricia Verástegui-Martínez [2], Sphyros Lastra [1] and Richard Solórzano-Acosta [1,3]

[1] Centro Experimental La Molina, Dirección de Supervisión y Monitoreo en las Estaciones Experimentales Agrarias, Instituto Nacional de Innovación Agraria (INIA), La Molina 1981, Lima 15024, Peru; slastrapaucar@gmail.com (S.L.); investigacion_labsaf@inia.gob.pe (R.S.-A.)
[2] Estación Experimental Agraria Santa Ana, Dirección de Supervisión y Monitoreo en las Estaciones Experimentales Agrarias, Instituto Nacional de Innovación Agraria (INIA), Carretera Saños Grande—Hualahoyo Km 8, Huancayo 12007, Peru; jvera@lamolina.edu.pe (J.V.-V.); patymarve@gmail.com (P.V.-M.)
[3] Facultad de Ciencias Ambientales, Universidad Científica del Sur (UCSUR), Lima 15067, Peru
* Correspondence: ricardo.floresm29@gmail.com

Abstract: *Ullucus tuberosus* is an Andean region crop adapted to high-altitude environments and dryland cultivation. It is an essential resource that guarantees food security due to its carbohydrate, protein, and low-fat content. However, current change patterns in precipitation and temperatures warn of complex scenarios where climate change will affect this crop. Therefore, predicting these effects through simulation is a valuable tool for evaluating this crop's sustainability. This study aims to evaluate ulluco's crop yield under dryland conditions at 3914 m.a.s.l. considering climate change scenarios from 2024 to 2100 by using the AquaCrop model. Simulations were carried out using current meteorological data, crop agronomic information, and simulations for SSP1-2.6, SSP3-7.0, and SSP5-8.5 of CMIP 6. The results indicate that minimum temperature increases and seasonal precipitation exacerbation will significantly influence yields. Increases in rainfall and environmental CO_2 concentrations show an opportunity window for yield increment in the early stages. However, a negative trend is observed for 2050–2100, mainly due to crop temperature stress. These findings highlight the importance of developing more resistant ulluco varieties to heat stress conditions, adapting water management practices, continuing modeling climate change effects on crops, and investing in research on smallholder agriculture to reach Sustainable Development Goals 1, 2, and 13.

Keywords: Andean tuber; *Ullucus*; climate change; AquaCrop; yield response

Citation: Flores-Marquez, R.; Vera-Vílchez, J.; Verástegui-Martínez, P.; Lastra, S.; Solórzano-Acosta, R. An Evaluation of Dryland Ulluco Cultivation Yields in the Face of Climate Change Scenarios in the Central Andes of Peru by Using the AquaCrop Model. *Sustainability* **2024**, *16*, 5428. https://doi.org/10.3390/su16135428

Academic Editors: Ioannis Mylonas, Fokion Papathanasiou and Elissavet Ninou

Received: 11 March 2024
Revised: 7 June 2024
Accepted: 10 June 2024
Published: 26 June 2024

1. Introduction

Tubers are important crops within Andean societies and their agro-food systems. They are characterized by their resilience to the region's adverse conditions. Among these crops, ulluco is prominent in food security due to its fundamental role in the Andean population's diet [1,2]. It is cultivated primarily in Peru, Bolivia, and Ecuador and is grown between 2000 and 4000 m.a.s.l. at temperatures between 11 and 13 °C [1–3]. Its nutritional contribution is based on its high carbohydrate content (64.96–84.2%), between 8.5 and 15.7% protein content, low-fat content (0.1–1.4%), fiber ranging 0.5–5%, and vitamin C [1,4,5]. Generally, tubers are boiled before eating. Nonetheless, they can also be dried to turn into *chuño* or milled into flour [6]. It is grown by more than 60 thousand producers in Peru, and during 2023, a cropping area of 42,912 ha with a 7.62 t·ha^{-1} average yield was reported, generating a total production of 173,116 t [7]. On average, dryland ulluco cultivation represents 82% of Peru's cropping area of ulluco, widely located in the Quechua and Sunni regions (94%). Monoculture patterns (86%) prevail over associations (14%) with crops such

as corn, mashua, potatoes, quinoa, etc. [8]. Even though its productive potential is less than other Andean tubers or roots [9], it is widely consumed in this region [1,10,11].

In the current context, climate change driven by carbon emissions from agriculture, livestock, industry, and households affects global agriculture through extreme weather events [12,13]. To research future impacts, the Working Group I (WGI) of the Intergovernmental Panel on Climate Change (IPCC) analyzed historical information and Global Climate Models (GCMs), generated as part of the Coupled Model Intercomparison Project (CMIP) to broaden our comprehension about the process and effects linked to climate change [14]. The fifth phase of the CMIP (CMIP5) analyzed future climatic projections based on Representative Concentration Pathways (RCPs), which express the increase in the most probable radiative forcing for 2100 [14]. Subsequently, the sixth phase's report provided different socioeconomic development pathways to achieve each RCP, thus proposing new levels of mitigation and adaptation actions to the effects of climate change [15]. These new scenarios are named Shared Socioeconomic Pathways (SSPs). SSP 1 and SSP 5 both propose increasing human development, differing in that the second proposes intensive fossil energy consumption as a means to achieve this; SSP 3 and SSP 4 propose pessimistic and inequitable development trends, while SSP 2 outlines continuity regarding historical patterns [14,15]. O'Neill et al. [15] identified priority analysis scenarios to update and cover information gaps of CMIP5 projections for RCPs—SSP1-2.6, SSP2-4.5, SSP3-7.0, and SSP5-8.5.

With all this information, it is possible to use existing models to explore potential yield changes in different crops. There are some experiences regarding modeling tuber and root growth such as potatoes, cassava, and sweet potatoes under diverse climates and water-available conditions [16–19]. Nevertheless, there is little research on crops in Andean regions [20–23] or on native crops such as ulluco [24–28], despite its importance for Andean food security and value in gourmet cuisine and industry.

AquaCrop is a model that simulates crop yields under different conditions based on plant water consumption; for this, it requires information about climate, crop, soil, and management conditions without considering pests' or diseases' potential effects [29]. Constant efforts are made to improve AquaCrop's simulation results while maintaining its simple modeling scope [30]. Due to its versatility, a wide range of research is linked to crop modeling through AquaCrop use for different climatic and management conditions, including climate change projections at different latitudes, longitudes, and altitudes [20,31,32]. At this point, the model's main limitations include its single-field-scale scope, assumptions of spatial uniformity inside the field, and the unidimensional vertical water fluxes simulated [33]. In addition, Vanuytrecht et al. [30] also outline the constant improvement of AquaCrop results to make them more accessible and understandable for agricultural extensionists, decision-makers, and stakeholders.

Several studies suggest that smallholding farming productivity in the Peruvian Andes is at imminent risk of decreasing due to water availability changes and increased temperatures [34–36]. The susceptibility of dryland crops to rainfall variability is exacerbated by changes in rainfall patterns due to climate change [34,37] which ultimately determines poverty conditions in rural areas [38]. Additionally, rising temperatures reduce the productive potential of crops adapted to cold regions [39]. This study focused on precipitation and temperature changes and their effect on ulluco yield.

Agronomic factors that influence tuber development have been investigated [40–43], as well as their potential food industry use due to their nutritional benefits [10,44–46] and their importance in local culture [47,48]. Ulluco's phenological development and productivity depend on climatic, edaphic, and genotypic factors, among others. Sowing dates are usually linked to rain presence in a crop rotation system with potatoes, oca, or barley [3,49].

Therefore, analyzing crop behavior facing extreme climate events is essential to develop adaptation strategies for different regional conditions [36]. This study evaluates the yield changes in *Ullucus tuberosus*, a key native Andean tuber, under dryland cultivation in

the Peruvian central highlands, according to climate change scenarios from the Coupled Model Intercomparison Project (CMIP) Phase Six for the 2024–2100 period.

2. Materials and Methods

2.1. Studied Area

This study was conducted in the town of San José de Apata, district of Apata, Jauja province, department of Junín, Peru. The experimental field was installed at 75°19′30.41″ W; 11°47′53.73″ S at 3914 m.a.s.l. (Figure 1). The area's climatic conditions are average annual precipitation, 689 mm; minimum temperatures between −4 °C (June–July) and 4 °C (March); maximum temperatures between 20 °C (March) and 22 °C (November–December); and average relative humidity, 72%. Averages were calculated based on historical data from Peru's National Service of Meteorology and Hydrology (SENAMHI) [50].

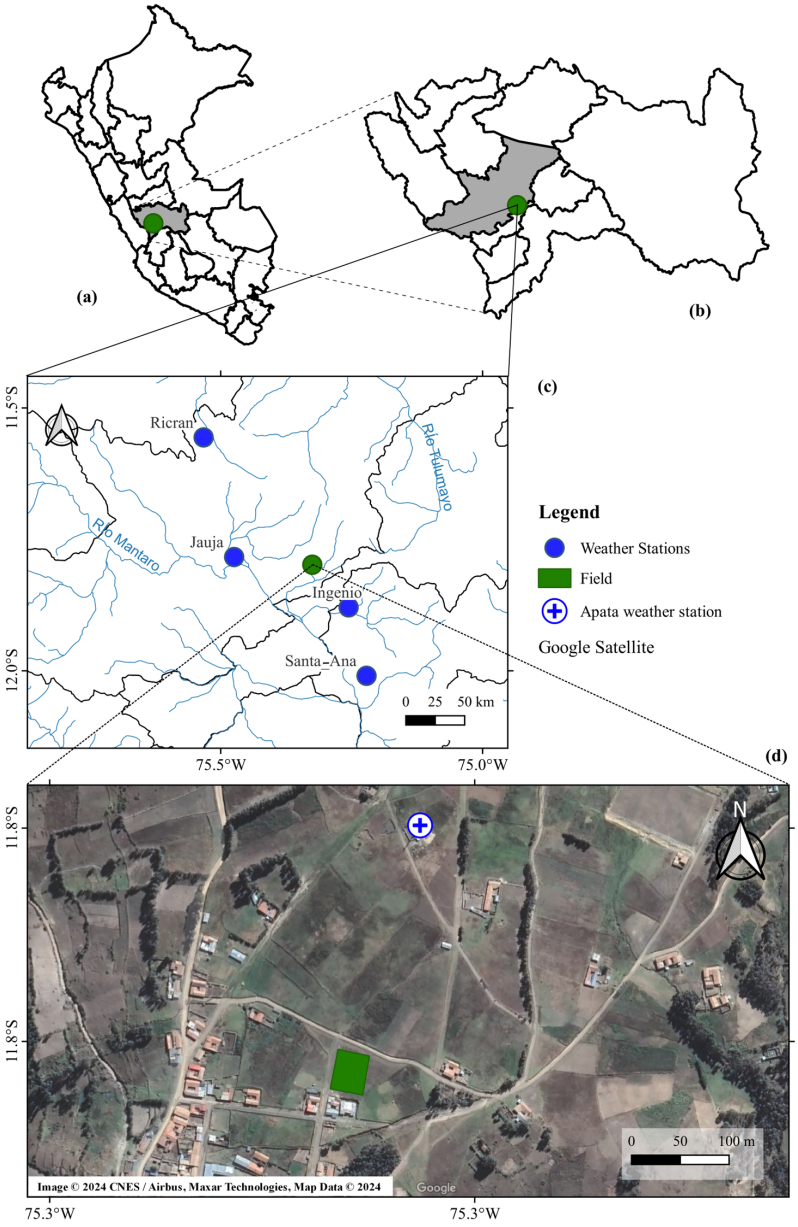

Figure 1. Studied area; (**a**) Junín department location within Peru; (**b**) Jauja province location; (**c**) location of the evaluation plot and meteorological stations used; (**d**) aerial satellite view of the evaluation plot.

2.2. Experimental Design

This study had a split-plot design in which the following two factors were tested: (i) sowing date (main plot with three levels) and (ii) the type of fertilization (sub-plot with two levels). Thus, six treatments with four replicates per treatment were used for 24 experimental units, as described in Table 1.

Table 1. Factors and levels tested.

Factor	Levels
Sowing date (F)	F1: 13 October 2022 F2: 28 October 2022 F3: 12 November 2022
Fertilization management (M)	M1: Traditional (sub-dose) * M2: Recommended (optimal dose) *

* Details of each fertilization management are described in Table of Section 2.5.

2.3. Experimental Plots Set-Up

Experimental plots were installed on a three-year fallow field where potatoes had previously been grown. *Ullucus tuberosus* cv. Canario was chosen due to its widespread cultivation in the central Peruvian Andes [51], sown at a density of 41,666 plants ha-1 (0.8 m × 0.3 m). A net plot consisting of 9 furrows, 6 m long, was established within each experimental unit. Data were collected from them. The spatial arrangement of the treatments can be found in Figure 2.

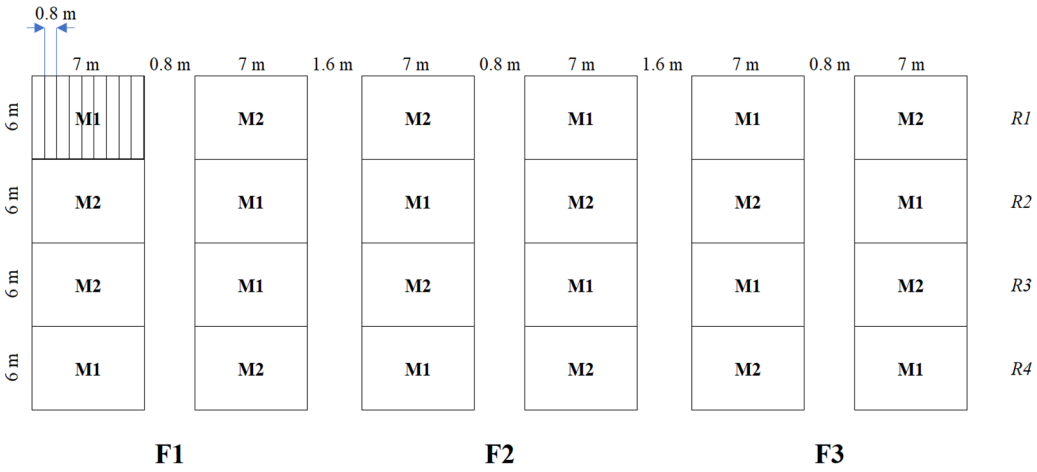

Figure 2. Field distribution of the experimental units.

2.4. Soil Characteristics

Before installation, a soil study was conducted in the experimental area. First, a soil pit was dug to a depth of 1.3 m, and, after observation, three horizons were determined, comprising topsoil (AP) and two strata of partially decomposed parent material (C1 and C2). For each of them, samples were taken and sent to the Soil, Water and Leaves Laboratory (LABSAF)—INIA Santa Ana to analyze bulk density (BD) [52], texture (Txt) [53], soil pH [54], electrical conductivity (EC) [55], organic matter (OM) content, nitrogen (N), phosphorus (P), potassium (K), and exchangeable aluminum (Al) [53] (Table 2). In addition, other soil samples were taken at the central zone of each evaluation unit, at 30 cm depth, to measure soil moisture content using the gravimetric method [56].

Table 2. Soil profile characterization.

Cod	Depth	pH	EC	OM	P	K	Al	N	Txt	BD
	m		$d \cdot Sm^{-1}$	%	$mg \cdot kg^{-1}$	$mg \cdot kg^{-1}$	$meq \cdot (100\ gr)^{-1}$	%		$g \cdot (cm^3)^{-1}$
AP	0.4	5.00	0.11	9.30	24.37	358.05	18.21	0.47	Loam	1.10
C1	0.65	4.92	0.07	1.15	2.24	54.61	19.50	0.06	Loam	1.38
C2	1.3	4.78	0.07	0.76	4.19	36.31	7.29	0.04	Sandy loam	1.80

Cod: horizon code, EC: electrical conductivity, OM: organic matter, P: phosphorus, K: potassium, Al: exchangeable aluminum, N: total nitrogen, Txt: texture, BD: bulk density.

2.5. Crop Fertilization

Fertilization was planned according to the second factor, proposed management (Table 1), considering the physical–chemical soil characterization results from the topsoil (Table 2). Details of the fertilization plan are shown in Table 3.

Table 3. Fertilization plan.

Management	Sheep Manure	Urea	DAF	ClK	Sulpomag	Agr Lime	Ammonium Nitrate
	$t \cdot ha^{-1}$	$kg \cdot ha^{-1}$	$kg \cdot ha^{-1}$	$kg \cdot ha^{-1}$	$kg \cdot ha^{-1}$	$kg \cdot ha^{-1}$	$kg \cdot ha^{-1}$
M1: Traditional	5.00	0	0	0	0	0	0
M2: Recommended	5.00	91.36	222.67	138.10	55.55	807.14	91.36

DAF: Diammonium phosphate; ClK: potassium chloride; Sulpomag: potassium and magnesium sulfate; Agr: Agricultural.

2.6. Weather Data

Weather data were obtained from a Davis Vantage Pro2 station managed by AGRORURAL located at 75°19′28.32″ W; 11°47′45.59″ S at 3950 m.a.s.l. Records included the whole growing season (2022–2023) (Figure 3).

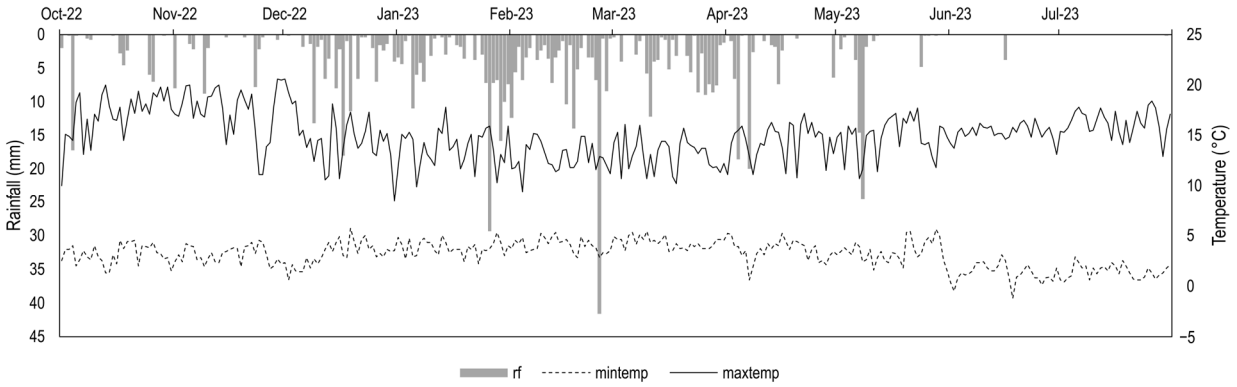

Figure 3. Apata station data for 2022–2023 on a daily scale. Rainfall (rf), maximum temperature (maxtemp), and minimum temperature (mintemp).

2.7. Data Collection of Morpho-Physiological Variables for Model Calibration

To calibrate the AquaCrop model, 9 evaluations were carried out during the whole growing season, starting from the phenological stage of emergence. In each one, five variables were assessed. In the phenological stage, direct observations of plants within furrow number 5 (the central 5 m of it) were performed. Plant canopy cover percentage was evaluated using RGB photographs taken with a NikonD3500 camera and processed with Image Canopy 3.6 and AutoCAD 2022 software. A total of 12 plants were assessed from each net plot (three plants from furrow numbers 2, 3, 7, and 8 each). The photographs were taken approximately 1 m above ground level. A square metal piece measuring 10 cm on a side was used as a measuring reference. Then, these plants were extracted from the

ground to measure their height and root depth. Finally, plant leaves were separated and prepared for dry matter analysis [16].

At the end of the season, samples were taken from the central 9 m^2 (3 m × 3 m) of the net plot to estimate the following crop-yield-associated variables: crop fresh weight, tuber dry matter, aerial and total dry matter, tuber dry matter (10 representative tubers per unit of assessment), and aerial and total dry matter (the sampled plants for yield) [16].

2.8. Statistical Analysis

Morpho-physiological variables were analyzed using a two-way ANOVA (alpha = 0.05) to examine treatment differences. Model assumptions were verified graphically with the autoplot function from the ggfortify library for R [57]. Variables that showed significant differences were analyzed with the Least Significant Difference Test (alpha = 0.05), LSD.test function from agricolae library for R [58], corrected with the Benjamini–Hochberg procedure.

2.9. AquaCrop's Crop Development Modeling

AquaCrop's climate input came from the weather station. It included rainfall data, maximum and minimum temperatures, wind speed, and relative humidity on a daily scale, which enabled the calculation of reference evapotranspiration (ETo) through the Penman–Monteith equation using the EToCalculator 3.2. The cropping module was completed with the image processing results from the canopy coverage analysis. Soil input values were determined with the information from the physical-chemical analysis of the soil pit. A management module was configured for dry conditions, weed management, fertilization, and furrowing characteristics. The iterative calibration process was based on the recommendations of [29], using calibrated parameters for potato cultivation from AquaCrop, the literature, and experts' opinions. The first simulation was performed with field-collected data (soil and weather). Missing parameters (conservative and non-conservative) were completed with available values in the literature, including those from potato crop research, which is extensive. Canopy cover data were adjusted for each phenological stage, considering the potential effects of heat and water stress. The impact of traditional fertilization (Table 1) was also considered. Calibration was performed considering the data from sowing dates 1 and 2 (Table 1). Model efficiency was evaluated through Pearson's correlation index (r) and the Nash–Sutcliffe efficiency index (NSE) for plant canopy coverage and crop yield data. The model was then validated with the data from sowing date 3 (Table 1), without changing the conservative parameters but adapting the sowing date. The model's efficiency was assessed using both previously mentioned indexes.

2.10. Climate Change Explorations

Since the weather station used for AquaCrop climate input does not have data before 2019, we used data from the SENAMHI network of weather stations [50]. The criteria for choosing proper data involved proximity to the experimental location and accessibility to historical data for rainfall (rf), maximum temperature (maxtemp), and minimum temperature (mintemp). Records from 1986 to 2017 were found. Downloaded data from four weather stations (Jauja: 75°29′12.73″ W–11°47′11.87″ S; Ingenio: 75°17′47.9″ W–11°52′30.8″ S; Ricran: 75°31′38.29″ W–11°32′24.05″ S; Santa Ana: 75°13′17.7″ W–12°0′34.4″ S) were homogenized, and missing registers were filled by the Paulhus and Kohler [59] method included in the Climatol package in R [60]. Subsequently, homogenized weather data for the experiment's geographical location were calculated using the weighted inverse distance interpolation method (WID) in Excel. Regarding climate change models, a total of 7 General Circulation Models (GCMs) belonging to the Coupled Model Intercomparison Project Phase 6 (CMIP6) were chosen (Table 4). The selection criteria involved prioritizing those evaluated for Peru and South America's conditions, in terms of their statistical downscaling adjustment [61,62]. GCM data corresponded to the historical period (1980–2014). To avoid the innate bias problems of the GCMs (over-estimation of minimum temperatures and

rainfall, as well as under-estimation of maximum temperatures) [62], after climate data extraction for plot location (using the terra package in R) [63], bias correction by quantile mapping was performed using the Qmap package in R [64]. Given our historical data, the model efficiency of all seven GCMs was evaluated to select the best-fitting model, based on Fernandez-Palomino et al. [62]. As a result of this analysis, the EC-Earth3 model was chosen to perform future projections, based on the Shared Socio-Economic Pathways' (SSPs) scenarios SSP1-2.6, SSP3-7.0 and SSP5-8.5, using the chosen model. The SSP1-2.6 scenario corresponds to a sustainable route, in which zero CO_2 emissions for the second half of this century are achieved. The SSP3-7.0 scenario considers doubled CO_2 emissions by 2100 due to regional rivalries and the absence of additional mitigation measures. The SSP5-8.5 scenario considers doubled CO_2 emissions by 2050 and the heavy use of fossil fuels to achieve human development. No further political measures are taken [14]. ETo was calculated using the Hargreaves method in the EToCalculator based on maximum and minimum projected temperature data for the selected model's future scenarios. To simulate ulluco yield for 2024–2100, rainfall, temperature, and ETo results were used as inputs for the climate module of the previously validated AquaCrop model, and atmospheric CO_2 concentration corresponded to the software database.

Table 4. Used CMIP6 models.

Model	Member	Historical (rf, Mintemp, Maxtemp)
IPSL-CM6A-LR	r14i1p1f1	[65]
CNRM-CM6-1	r1i1p1f2	[66]
CNRM-ESM2-1	r1i1p1f2	[67]
MIROC6	r50i1p1f1	[68]
MRI-ESM2-0	r5i1p1f1	[69]
MPI-ESM1-2-HR	r2i1p1f1	[70]
EC-Earth3	r150i1p1f1	[71]

3. Results

3.1. Tuber Yields by Sowing Date and Type of Fertilization

In addition to modeling, whether the tested variables influenced ulluco's yield was determined, as shown in Table 5.

At the main effects level, the sowing date (F) had no significant effect on fresh and dry weight yield, nor the number of tubers per kilogram. On the other hand, the fertilization method significantly affected the three evaluated variables for ulluco. The recommended dose values doubled under conventional management conditions in fresh weight (FW) and dry weight (DW) cases. It was found that yield decreases the later the sowing date takes place. However, mineral fertilization efficiency also decreases because less water is available as the sowing date is delayed (Table 5). Its efficiency is similar to traditional manure fertilization (Figure 4). The cumulative rainfall for the F1 growing season was 677 mm, 657 mm for F2, and 635 mm for F3.

Table 5. Ulluco tuber's yield by sowing dates and type of fertilization.

Treatment	Fresh Weight Yield ($Mg \cdot ha^{-1}$)	Dry Weight Yield ($Mg \cdot ha^{-1}$)	Number of Tubers per kg
F	ns	ns	ns
M	***	**	***
F × M	*	ns	ns

Table 5. *Cont.*

Treatment		Fresh Weight Yield (Mg·ha^{-1})	Dry Weight Yield (Mg·ha^{-1})	Number of Tubers per kg
Sowing Date (F)				
F1		10.50 ± 5.0	1.28 ± 0.6	117.7 ± 24
F2		9.53 ± 6.8	1.10 ± 0.8	102.6 ± 27
F3		8.41 ± 1.6	1.16 ± 0.3	108.2 ± 17
Fertilization Method (M)				
Traditional (M1)		6.4 ± 2.3 ^{b}	0.77 ± 0.3 ^{b}	123.0 ± 22 ^{a}
Recommended (M2)		12.56 ± 4.7 ^{a}	1.59 ± 0.5 ^{a}	96.0 ± 15 ^{b}
F × M				
F1	M1	6.8 ± 2.8 ^{c}	0.79 ± 0.3	135.38 ± 20.9
	M2	14.2 ± 3.7 ^{a}	1.77 ± 0.5	100.06 ± 5.7
F2	M1	5.0 ± 2.7 ^{c}	0.57 ± 0.3	111.96 ± 30.1
	M2	14.1 ± 6.8 ^{ab}	1.64 ± 0.8	93.14 ± 24.2
F3	M1	7.4 ± 0.5 ^{bc}	0.96 ± 0.1	121.7 ± 7
	M2	9.4 ± 1.9 ^{abc}	1.36 ± 0.3	94.7 ± 12

*** Implies statistical significance at 0.1%; ** implies statistical significance at 1%; * implies statistical significance at 5%; ns: indicates not significant ($p > 0.05$); different letters in each testing parameter represent statistical significance among groups at $p < 0.05$ for Tukey Test.

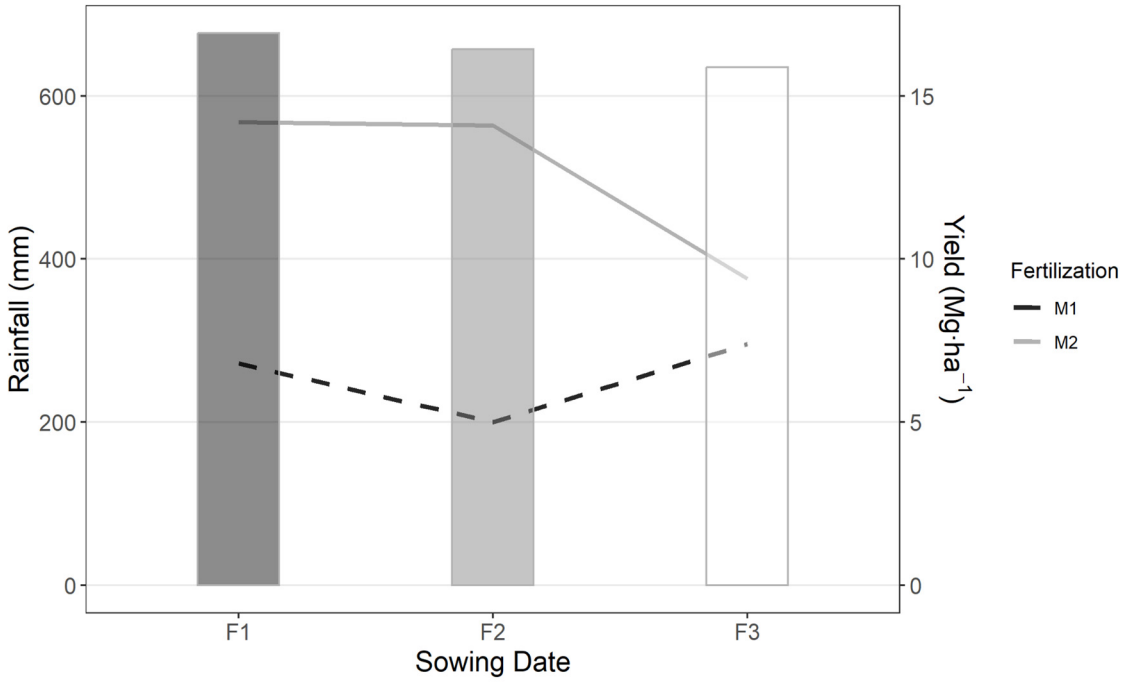

Figure 4. Bar graph showing rainfall (mm); and line graph showing marginal means of fresh weight yield of ulluco by sowing date (F1: 13 October 2022, F2: 28 October 2022, F3: 12 November 2022) response, and fertilization management (M1: traditional, M2: recommended).

3.2. Ullucus Tuberosus Cultivation Development Model under Dryland Conditions

The 2022–2023 season was characterized by wetter rainy season, maximum temperatures below the historical average, and minimum temperatures similar to the historical average, even reaching below 0 °C in the last months of the crop's phenological development (Figure 5). The F1M2 and F2M2 field data allowed for the model's calibration of conservative parameters in AquaCrop. Efficiency values for this phase of r: 0.99, NSE: 0.98, and r: 0.91—NSE: 0.82 were obtained for F1 and F2 plant coverage, respectively. Generated

canopy cover curves from the parameterization are shown in Figures 6 and 7, showing the model's slight difficulty in reaching the maximum plant coverage of F2 (simulated canopy cover [CCsim] vs. observed canopy cover [CCobs]). In the next step, based on the obtained parameters, the model was validated with F3M2 data, obtaining efficiency indicators of r: 0.94 and NSE: 0.88 (Figure 8). The AquaCrop model calibrated parameters are shown in Table 6.

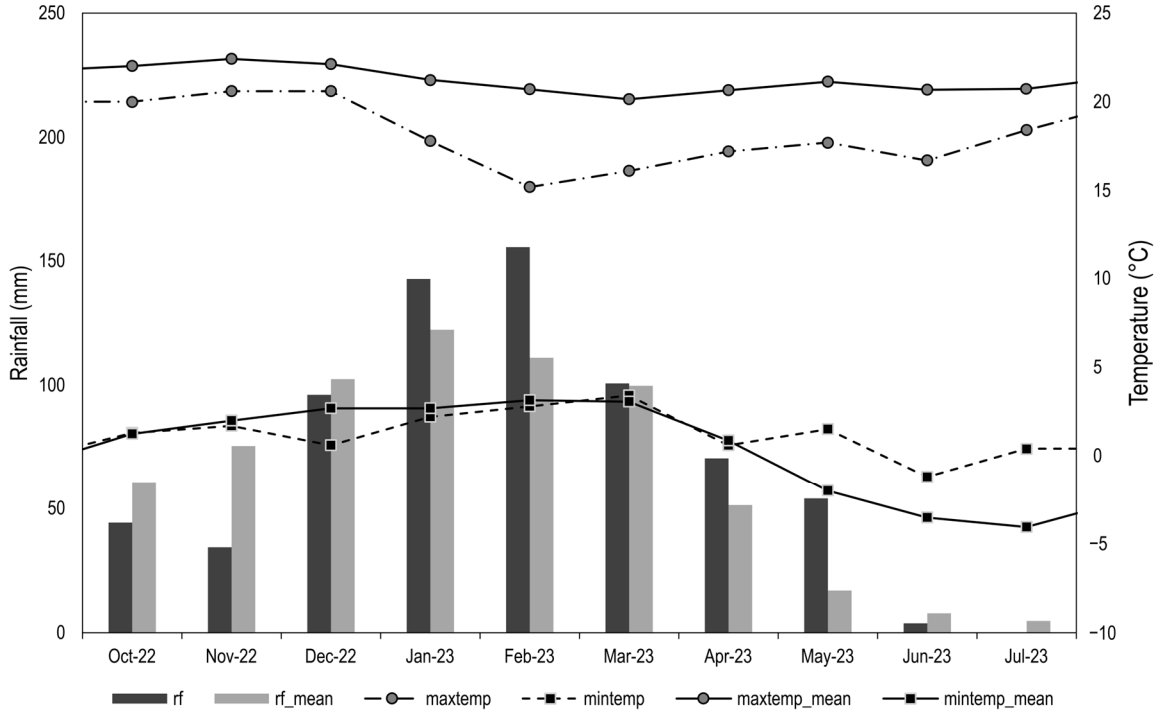

Figure 5. Apata station data (2022–2023) and historical averages on a monthly scale. Rainfall (rf), maximum temperature (maxtemp), and minimum temperature (mintemp).

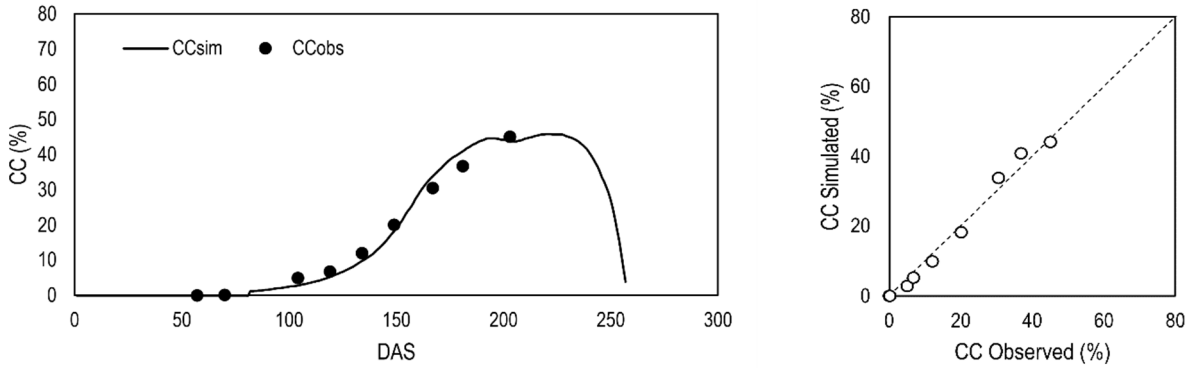

Figure 6. F1M2 calibration. DAS: days after sowing. CC: canopy cover. CCsim: simulated canopy cover. CCobs: observed canopy cover.

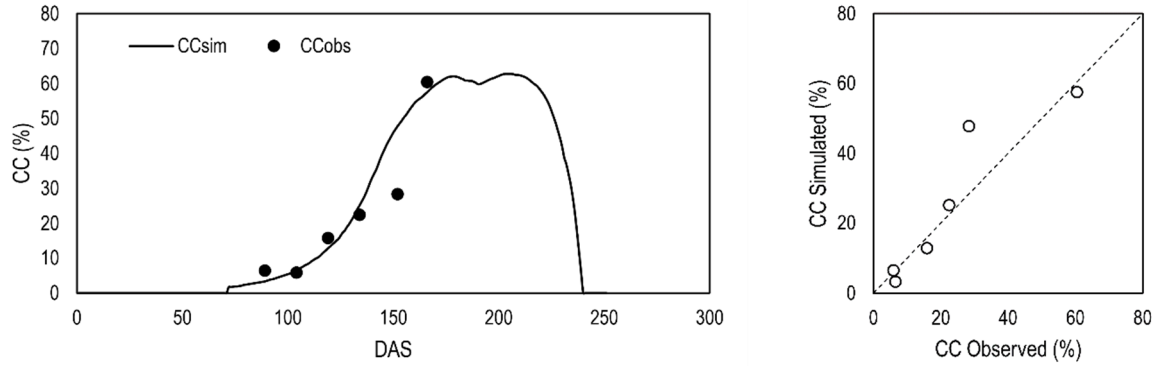

Figure 7. F2M2 calibration. DAS: days after sowing. CC: canopy cover. CCsim: simulated canopy cover. CCobs: observed canopy cover.

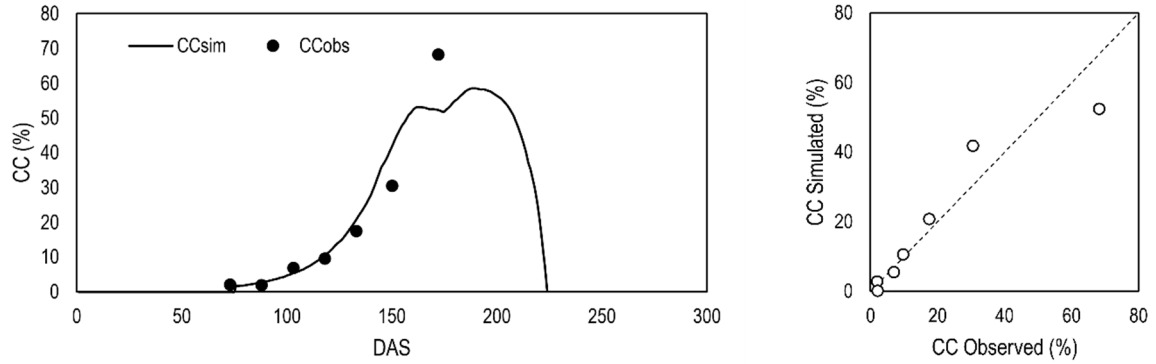

Figure 8. F3M2 validation. DAS: days after sowing. CC: canopy cover. CCsim: simulated canopy cover. CCobs: observed canopy cover.

Table 6. AquaCrop model parameter calibration for ulluco dryland crop.

Parameter	Initials	Value	Unit	Method of Determination	Base Literature
Development					
Plant density		41,667	plant ha^{-1}	M	[1]
Canopy development					
Canopy growth coefficient	CGC	0.677	% GDD^{-1}	C	[9]
Canopy decline coefficient	CDC	1.337	% GDD^{-1}	C	[9]
Root deepening					
Max effective rooting depth		0.25	m	M	
Average root zone expansion		0.1	cm day^{-1}	D	
Minimum effective rooting depth		0.2	m	E	
Shape factor of root deepening		1.5		D	
Evapotranspiration					
Soil evaporation					
Effect of canopy shelter in late season		60	%	D	
Crop transpiration	Kc tr,x	1.15		D	
Aging		0.15	% day^{-1}	D	
Water extraction pattern		40–30–20–10	%	D	
Production					
Normalized Water Productivity	(WP*)	13	g m^{-2}	L	[16]
Adjustment for yield formation		77	% of (WP*)	L	[16]
Performance under elevated CO_2					
Sink strength		50	%	D	
Reference Harvest Index	HIo	60	%	C	[9]
Composition of fresh yield					
%water		85	%	C	[2,9]
% dry matter		15	%	C	[2,9]

Table 6. *Cont.*

Parameter	Initials	Value	Unit	Method of Determination	Base Literature
Water stress					
Canopy expansion					
p (upper)		0.3		E	[1,72]
p (lower)		0.65		E	[1,72]
shape factor		3		D	
Stomatal closure					
p (upper)		0.6		D	
shape factor		3		D	
Early canopy senescence					
p (upper)		0.7		D	
shape factor		3		D	
Temperature stress					
Base temperature		2	°C	E	[1,43]
Upper temperature		26	°C	E	[1,43]
Crop transpiration affected by cold stress					
Full stress		0	°C		
No stress		7	°C	D	[1,43]
Fertility stress					
CCx reduction		47	%	C	
CGC reduction		16	%	C	
Average decline canopy cover		0.2	% day^{-1}	C	
WP* reduction		25	%	C	
Salinity stress				NA	

C: calibration; D: AquaCrop default for potato; E: estimation; L: literature; M: measured; NA: not applicable. GDD: growing degree days; CCx: maximum canopy; Kc tr,x: coefficient for maximum crop transpiration, WP*: normalized water productivity. Note: gray hatched cells are conservative parameters.

The modelled/measured fresh weight yield was F1: 13.8 t·ha^{-1}/15.28 t·ha^{-1}, F2: 14.9 t·ha^{-1}/17.36 t·ha^{-1}, and F3: 9.19 t·ha^{-1}/10.23 t·ha^{-1}, while the modelled/measured dry weight yield was F1: 2.07 t·ha^{-1}/1.86 t·ha^{-1}, F2: 2.23 t·ha^{-1}/2.02 t·ha^{-1}, and F3: 1.38 t·ha^{-1}/1.49 t·ha^{-1}.

3.3. Climate Change Scenarios

Bias correction was performed for the three variables of interest in the historical period per station, and extreme values were represented (Figure 9). The EC-Earth 3 model was selected from which projected data bias for the 2015–2100 period was extracted and corrected for the SSP1-2.6 [73], SSP3-7.0 [74], and SSP5-8.5 [75] scenarios (Figure 10).

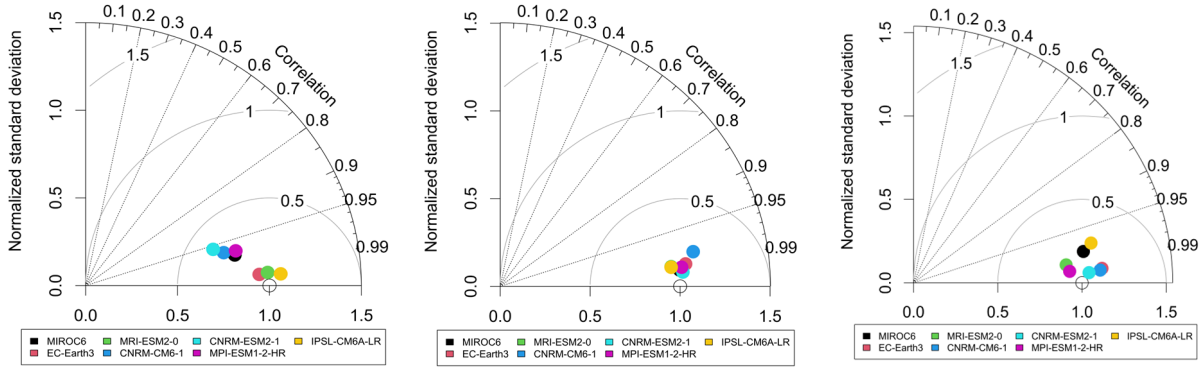

(**a**) (**b**) (**c**)

Figure 9. Taylor diagrams for extreme values of GCM historical corrected data; (**a**) rainfall above the 95th percentile of analyzed values; (**b**) under 5th minimum temperature percentile of analyzed values; and (**c**) above 95th maximum temperature percentile, evaluating monthly aggregates.

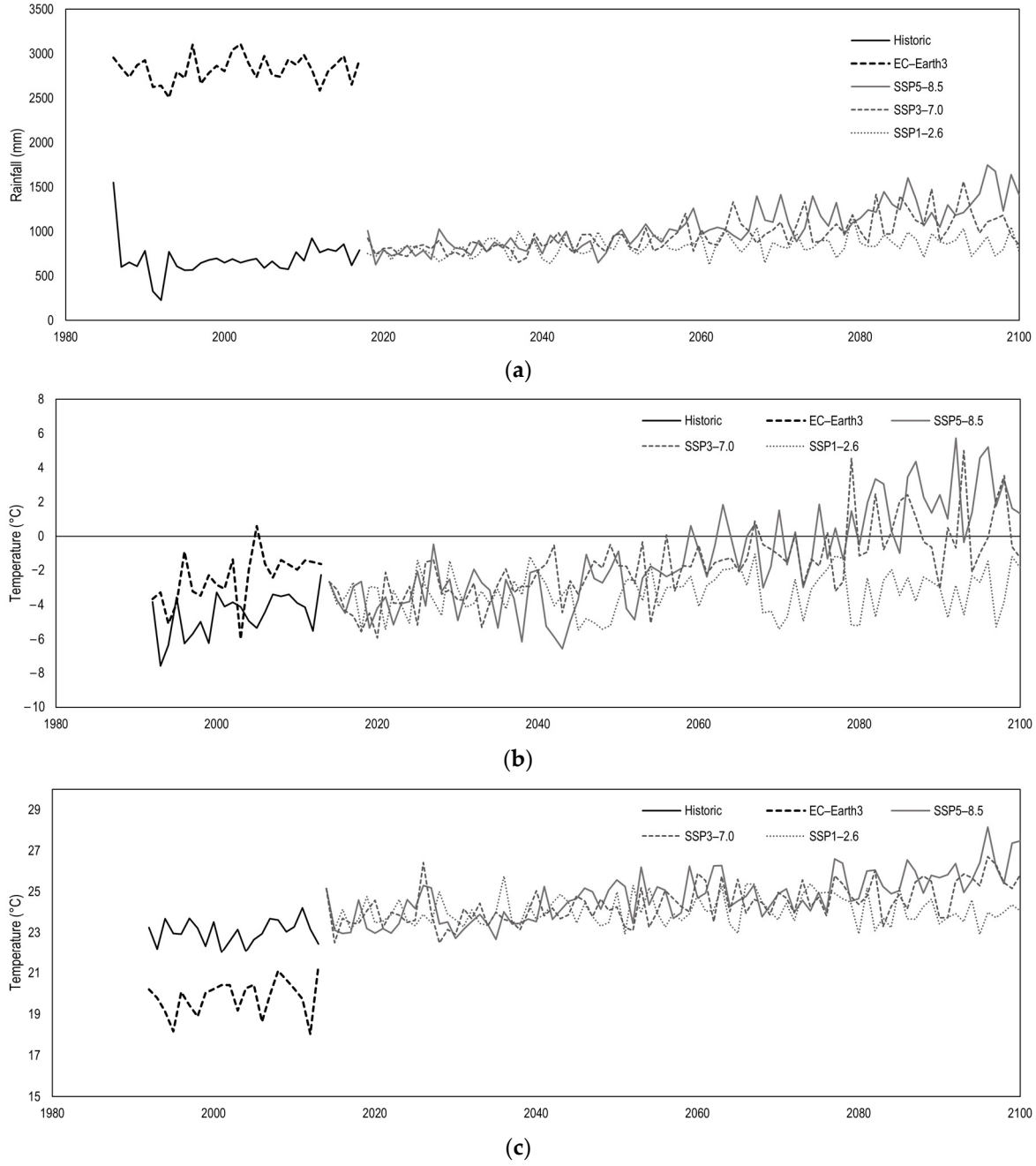

Figure 10. Climate variables projection for SSP126, SSP370, and SSP585 from corrected data of EC-Earth3; (**a**) rainfall; (**b**) minimum temperature; (**c**) maximum temperature. Annual scale grouping for the three variables.

Regarding the three analyzed scenarios (SSP1-2.6, SSP3-7.0, and SSP5-8.5) it is possible to observe that the EC-Earth 3 model projects an increasing trend in cumulative annual precipitation. In the last projected third (2075–2100), mean monthly value differences between the dry and wet seasons are accentuated (Figure 11a). On the other hand, increases in minimum and maximum temperature are observable for the three analyzed scenarios with an emphasis on the dry season (June–October) and for the minimum temperature.

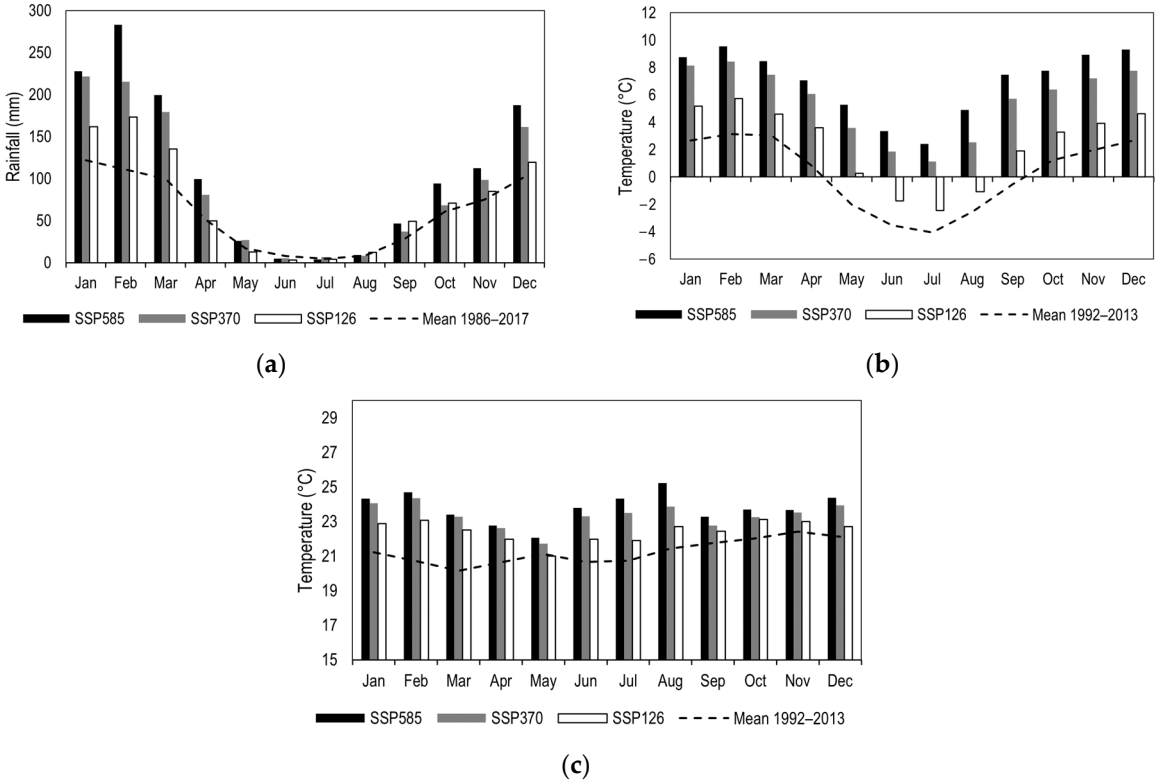

Figure 11. Monthly average values for the 2075–2100 period for SSP126, SSP370, and SSP585 from the EC-Earth3 model, in contrast to the observed historical average; (**a**) rainfall; (**b**) minimum temperature; (**c**) maximum temperature.

3.4. Yield Projections under Climate Change Conditions

The assessment results show that climate change significantly impacts ulluco yields under dryland conditions. Projections suggest a rainfall increase, accentuating differences between dry and rainy seasons, and temperature increase, mainly in the minimum temperatures. Regarding F1 and F2 conditions, a decrease in variability is observed in yield towards the last projected third in SSP1-2.6, while yield variability persists in SSP3-7.0. By contrast, a decreasing tendency toward projected yield is observed from the middle of the analysis period in SSP5-8.5. Regarding F3, it is observed that for the SSP1-2.6 scenarios, there is higher yield variability compared to SSP3-7.0 and SSP5-8.5. However, for the second half of the analysis period, this changes. In SSP1-2.6 and SSP3-7.0, a trend towards more constant yields is noted, while in SSP5-8.5, a decreasing trend is observed from the middle of the 2024–2100 period.

In all evaluated scenarios, there is a prevalence of F3 achieving higher yields compared to F1 and F2, as well as a lower failed campaign percentage (F1: 18%; F2: 13%; F3: 6%). However, an initial trend of slightly increasing yields is identified followed by a negative trend from the projection period's latter half.

4. Discussion

This study aimed to assess three climate change scenarios and their impact on the productivity of ulluco crops. To achieve this, historical weather data on rainfall and temperature were used to simulate changes from 2024 to 2100. Results from these simulations and data collected from the experimental plots were used as inputs for the required modules of the AquaCrop model. It is important to mention that the chosen area very well represents the conditions of a typical ulluco-producing area in a rainy, cold climate with dry autumns and winters [76]. Therefore, the results of this study are relevant for growing areas at the same altitude and similar soil conditions in the Andean region.

The results of the climate change simulations indicate an increasing trend in accumulated rainfall for the period 2024–2100 for three scenarios (Figure 10). Our findings contrast with those of Wongchuig et al. [77], who forecasted a reduction in annual precipitation for the same period in the Suni and Quechua regions of the Mantaro River basin. Arana et al. [78] found that historical data from the Jauja, Ingenio, and Ricrán weather stations also showed an ascending pattern. Seeing such discrepancies in the forecasts is expected because the complexity of the Andean topography largely influences bias correction processes [62] as a result of constantly changing thermal and moisture fluxes [79]. An important finding in our results was that in the last 25 years of this century, the distribution of rain throughout the year will remain similar in the sense that June, July, and August will remain predominantly dry, and the increase in cumulative precipitation will be allocated during the wet season. In other words, the rainy season will be rainier, especially in December, January, February, and March (Figure 11). This finding is in line with that of Almazroui et al. [61] who indicate stronger seasonality for this century's last period. The simulations suggest a sharp increase in minimum temperatures (Figure 11), especially for the SSP585 and SSP370 scenarios, which are the most concerning regarding climate change mitigation. Maximum temperatures seem to remain similar. All this is in accordance with the historical trends analyzed by Arana-Ruedas et al. [78] and Sanabria et al. [38], who explained that temperature increases in the studied area will be more pronounced for the minimum rather than maximum values but without concluding that frost damages in crops will necessarily be more harmful due to the complexity of this process.

The results of the AquaCrop simulations indicate that the latest sowing date, F3 (Table 3), will have a better fresh weight yield (Figure 12) in all three scenarios, and, on average, would have a greater increase in fresh weight yield concerning the 2022–2023 season's base yield (Figure 13). Given that the maximum temperatures will most likely remain constant, the underlying explanation can be found in minimum temperature and precipitation changes, specifically from 2075 to 2100 (Figure 10). The optimum temperature for ulluco has been studied as ranging between 11 and 13 °C [1]. In this sense, warmer minimum temperatures will affect the daily temperature average, impacting the duration of phenological transitions [80]. This indicates that the cropping period can be shortened, which could detrimentally affect yields. On the other hand, this species needs a low-temperature stimulus to start forming tubers [41]. If late sowing occurs in mid-November, tuberization induction is expected to happen by the end of February, when minimum temperatures reach 2°C under current conditions (Figure 11). All three scenarios forecast that minimum temperatures will be between 5 and 10 °C, which could affect tuber formation. In addition, maximum temperatures are expected to become 2 degrees higher during the tuber filling stage (March and April) (Figure 11), adding extra physiological problems, as it could even exceed the optimum range of 11–13 °C. Wahid et al. [81] define heat stress as plant growth and development limitations, caused by an air temperature increase above the optimal crop temperature, for a sufficient period to cause damage. Sage et al. [82] mention that between 5 and 6 °C increases in the plant's optimal temperature generate dry matter accumulation inhibition in reserve organs and greater infection susceptibility to pathogens. Likewise, high temperatures in heat-sensitive plants cause stomatal conductance decrease, CO_2 fixation inhibition, and oxidative damage in photosystem II [83,84]. It is important to consider how temperature increase involves an increase in incidences of pests and diseases [72]. Unfortunately, AquaCrop does not incorporate these effects in its calculations [29], so we should be critical regarding this factor.

On the other hand, the fact that wet seasons are expected to become rainier (Figure 11) might positively affect the early stages of plant development. This can be associated with the results of the experimental plot (Figures 6–8), in which plant emergence at early sowing treatments (Figure 6) took place 53 days after sowing, in comparison with normal sowing (Figure 7) and late sowing (Figure 8), which took place at 90 and 75 days, respectively. By relating this phenological transition with rainfall registered at the weather station (Figure 3), we can see that an intense precipitation event before early sowing (13 October 2022) was

the single different weather variable compared to the other two sowing dates. On the other hand, during October and November, when sowing of the two latest treatments took place, only 34–44 mm of accumulated rainfall and around 8.6 °C average temperatures were recorded, which may have influenced the emergence delay of the last two sowing date treatments [49]. This suggests that more significant water availability may be beneficial for accelerating canopy emergence, which is a crucial factor in guaranteeing crop success. Despite this positive effect of water availability at the early stages of the crop, it is important to mention that an even distribution of precipitation is crucial, particularly after tuber induction, which usually takes place 90 days after sowing. Unfortunately, during April and May 2023, when tubers fill in, precipitation decreased drastically compared to February and March (Figure 3). This might be why the late sowing treatment at optimum fertilization rates performed worse than the other two treatments. This indicates the importance of having good soil moisture content during the filling stage. Fertilization proved to play a differentiating role when water was available (Figure 4). On its own, proper fertilization doubled yields compared to the traditional way, which far exceeds that reported by Nieto-Cabrera et al. [85] who indicated an 18.5% increase due to fertilization effects. However, if there is a water shortage during the filling stage, fertilization becomes an irrelevant factor, as the yields will be similar to plots that are not fertilized (Figure 4). The experimental plots yielded results comparable to those described by Sánchez-Portillo et al. [1], in which 2–10 $t \cdot ha^{-1}$ were obtained under Ecuadorian conditions. In addition to this, fresh and dry weight relations coincided with the high-water content expected for this tuber (72–87%) [2,9]. However, our fresh yield results were far from the optimal of 26 t ha^{-1}, as reported by Condori et al. [9] for irrigated ulluco crops, under Bolivian highland conditions. This yield gap between irrigated ulluco crops and dryland ones indicates how susceptible this crop is to the lack of a proper water supply. Although the models predict an increasing trend of accumulated precipitation over the years (Figure 10), it is not certain that such volumes will be evenly distributed during the growing season, or most importantly, that they will take place during periods of higher water demand for the crop (emergence and tuber filling).

All in all, this exploratory study alerts stakeholders and decision-makers to the necessity of strategically planning how to address the previously mentioned problems (i.e., temperature increases and excess water in the soil during future rainy seasons). Water management practices such as rain harvesting can be considered a way of storing excessive rainwater, and complimentary irrigation systems can prevent water shortage during critical phenological stages. On the other hand, excessive soil moisture could damage the crop; therefore, drainage systems can be included in plots that become easily flooded. Furthermore, this is an opportunity to suggest future plant breeding programs that allow for tuberization at higher temperatures and achieve heat stress-resistant cultivars.

The findings of this study highlight the susceptibility of ulluco, a native tuber, to climate change. Extrapolation of this potential effect to other minor native tubers due to their characteristic long growth cycles [86] can predict a shift in cultivated crops in highlands. It could increase the production costs, the loss of traditional field management, and the disruption of native crop roles in agroecosystems [86]. Losing traditions of native crop management such as crop rotation could cause soil health degradation, jeopardize agrobiodiversity conservation, and emphasize poverty patterns due to the settled subsistence of the agriculture–poverty relation [87]. Therefore, building the resilience of the local food system and investing in research on smallholder agriculture will be critical for reaching Sustainable Development Goal (SDG) 2 (Zero hunger) and SDG 1 (No poverty) [87]. In addition, the good performance of AquaCrop to model tubers allows us to perform climate change impact predictions to improve national climate change adaptation policies toward SDG 13 (Take urgent action to combat climate change and its impacts).

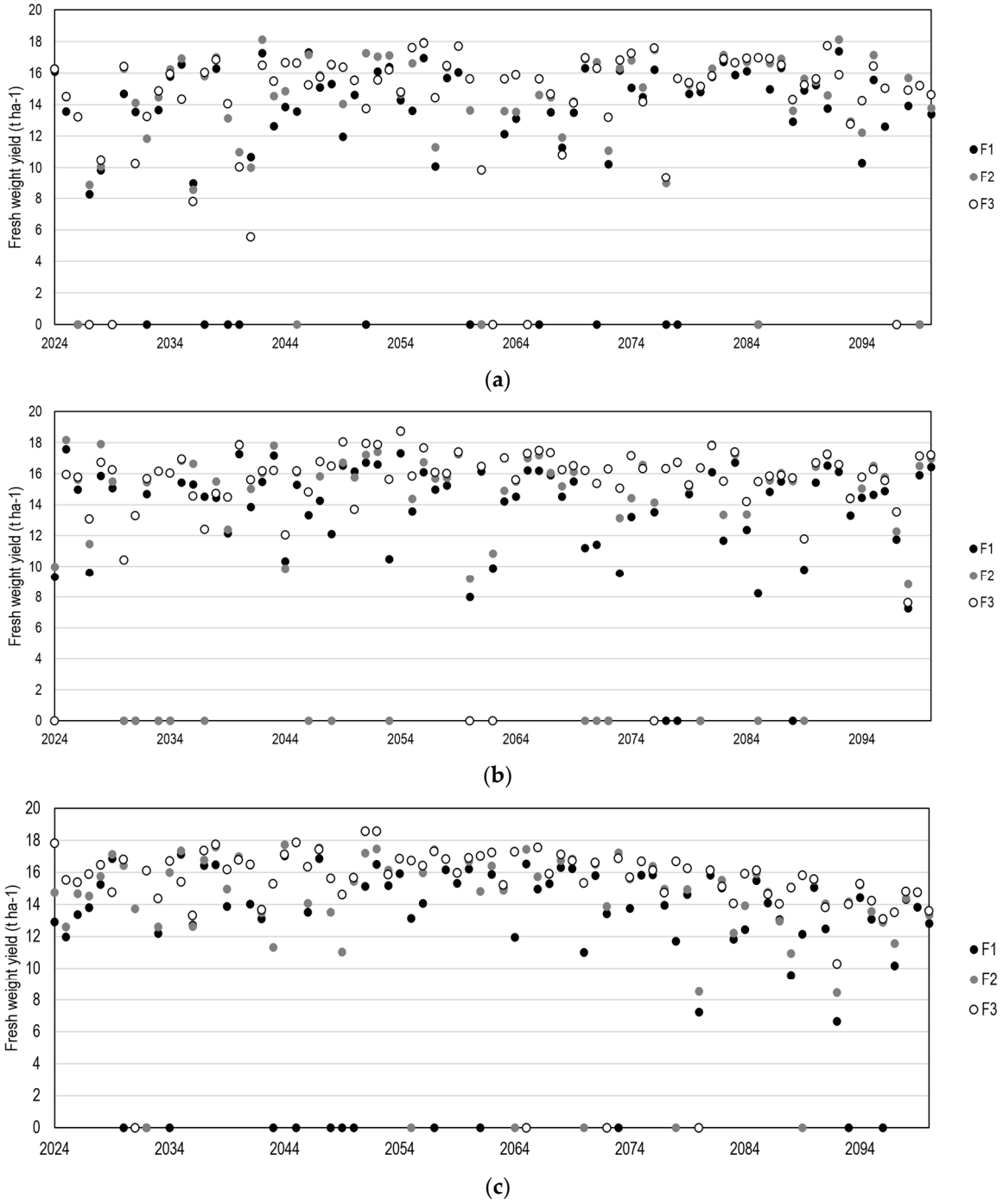

Figure 12. Ulluco's fresh weight yields (t·ha^{-1}) projected for (**a**) SSP1-2.6; (**b**) SSP3-7.0; and (**c**) SSP5-8.5 considering the three sowing dates (F1: 13-oct, F2: 28-oct, F3: 12-nov).

In addition, some policy suggestions are presented comparing this study and the strategic actions proposed in Peru's National Adaptation Plan Against Climate Change [88]. Modeling studies should be increased to broaden the prediction of possible climate change effects on critical food security crops and regional agrobiodiversity conservation. This measure can enhance the performance of early warning services and the scope of agro-climatic risk forecasts. However, in Peru, the results of the forecasting service developed by SENAMHI have restricted scope due to the limited Internet connection in the highlands [89] and the short list of commercial crops analyzed [90]. Furthermore, the water resources management policies for highlands should focus on Natural Infrastructure and

Water Sowing and Harvesting (WSH) due to their more straightforward and lower-cost implementation process and easier adaptation to local traditional practices. Therefore, the more democratic the construction of knowledge is, the easier it will be for farmers to adopt proposed policies and technologies.

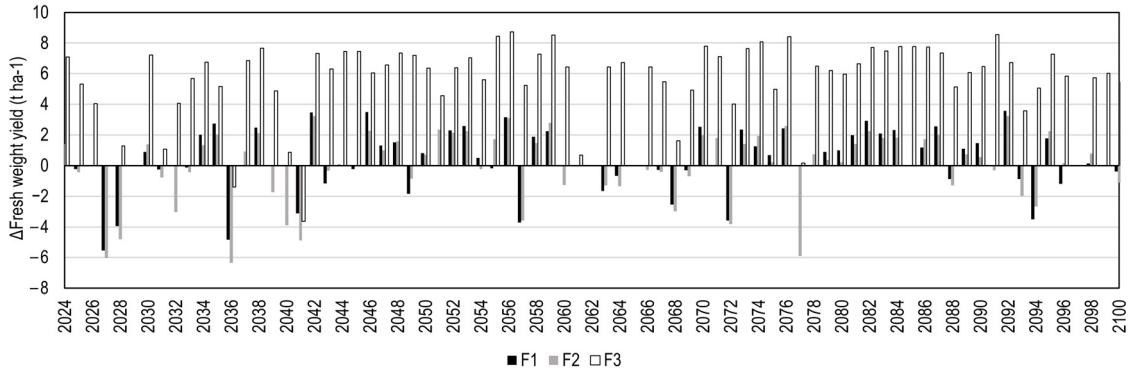

(**a**)

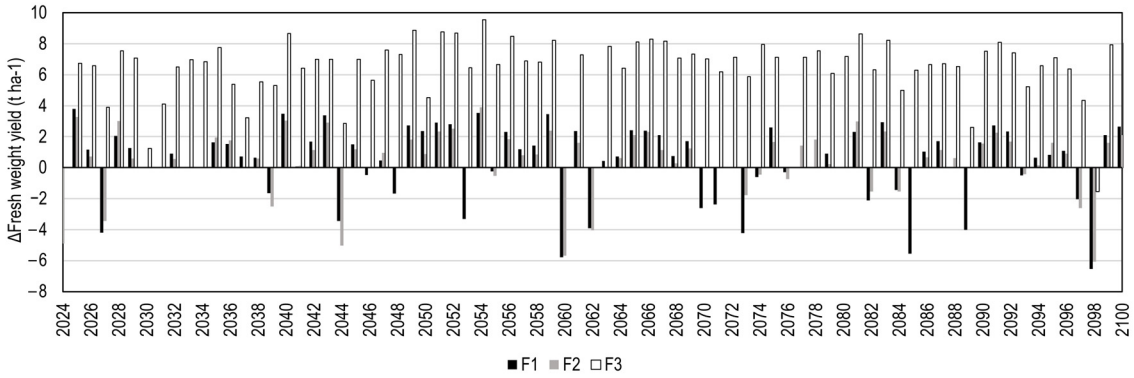

(**b**)

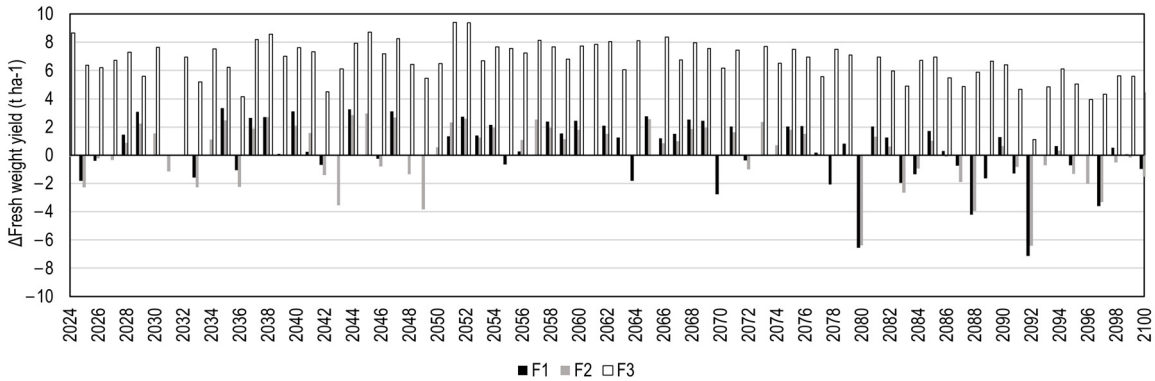

(**c**)

Figure 13. Ulluco's fresh weight yield (t·ha^{-1}) variations projected concerning the 2022–2023 season's base yield for (**a**) SSP1-2.6; (**b**) SSP3-7.0; and (**c**) SSP5-8.5 considering the three sowing dates (F1: 13-oct, F2: 28-oct, F3: 12-nov).

5. Conclusions

The AquaCrop model adequately represents ulluco cultivation development under dryland conditions for Peru's central highlands, allowing for yield projection analysis and crop management for changing environmental conditions. In this context, GCM analysis corresponding to CMIP 6 outlined how the more substantial mitigation and adaptation measures scenario (SSP1-2.6) projects an increase of up to 50% in precipitation for the rainy

season in the period 2075–2100 and an average increase of 2 °C for minimum temperature. The maximum temperature in the rainy season (January–March) will increase regardless of mitigation and adaptation measures. By contrast, extreme values in the dry season (June–August) will be directly related to adopted measures on climate change—more intense for SSP5-8.5 and SSP3-7.0. Thus, for the intensive fossil fuel scenario (SSP5-8.5), maximum temperatures will reach 24–25 °C peaks, and minimum temperatures will increase sharply by 2050 with increases of up to 6 °C and exceeding 0 °C. These changes in maximum and minimum temperatures will impact ulluco's yield. In addition, for pessimistic scenarios (SSP5-8.5 and SSP3-7.0), rainfall in the rainy season can double the historical monthly precipitation volume, which means more intense events with greater erosive potential.

Increases in rainfall and environmental CO_2 concentrations show an opportunity window for yield increment in the early stage of the 2024–2100 period. However, in very high greenhouse gas concentration scenarios, a negative trend is observed for 2050–2100 mainly due to crop temperature stress, increased soil evaporation, and crop transpiration. A trend toward yield stability is achieved throughout the projected period for more optimistic scenarios. In summary, evaluating dryland ulluco cultivation yield under climate change scenarios using the AquaCrop model highlights the urgency of mitigating potential negative impacts on this agricultural system. This study remarks on the importance of carrying out adaptive sustainable practices concerning climate change such as rain harvesting for storing the excessive amount of rainwater and complimentary irrigation systems to prevent water shortage during critical phenological stages; the continuity of modeling future climate change effects to improve the information for agroclimatic risk forecast; the recommendation to plan plant breeding programs looking for tuberization at higher temperatures and heat stress-resistant cultivars; or investing in research on smallholder agriculture to reach SDG 1 and SDG 2.

Author Contributions: R.F.-M., conceptualization, methodology, validation, writing—original draft, visualization, investigation; J.V.-V., conceptualization, methodology; P.V.-M., methodology; S.L., writing—review and editing; R.S.-A., supervision, writing—review and editing. All authors have read and agreed to the published version of the manuscript.

Funding: This research was funded by the CUI 2487112 INIA project "Research and technology transfer services improvement in the management and recovery of degraded agricultural soils and irrigation water for small and medium-scale agriculture in the departments of Lima, Ancash, San Martín, Cajamarca, Lambayeque, Junín, Ayacucho, Arequipa, Puno, and Ucayali".

Institutional Review Board Statement: Not applicable.

Informed Consent Statement: Not applicable.

Data Availability Statement: The data presented in this study are available on request from the corresponding author.

Conflicts of Interest: The authors have no conflicts of interest to declare.

References

1. Sanchez-Portillo, S.; del Sánchez, M.R.S.; Solanilla-Duque, J.F.; Herrera, R.R. Andean Tubers, Morphological Diversity, and Agronomic Management: A Review. *Plant Sci. Today* **2023**, *10*, 98–105. [CrossRef]
2. Manrique, I.; Arbizu, C.; Vivanco, F.; Gonzales, R.; Ramírez, C.; Chávez, O.; Tay, D.; Ellis, D. *Ullucus Tuberosus Caldas: Colección de Germoplasma de ulluco Conservada en el Centro Internacional de la Papa (CIP)*, 1st ed.; International Potato Center: Lima, Peru, 2017; ISBN 978-92-9060-482-2. [CrossRef]
3. Tapia Núñez, M.E.; Fries, A.M.; Mazar, I. *Guía de Campo de los Cultivos Andinos*, 1st ed.; Rosell, C., Ed.; Asociación Nacional de Productores Ecológicos del Perú: Lima, Roma; Organización de las Naciones Unidas para la Agricultura y la Alimentación: Lima, Roma, 2007; ISBN 978-92-5-305682-8.
4. Busch, J.M.; Sangketkit, C.; Savage, G.P.; Martin, R.J.; Halloy, S.; Deo, B. Nutritional Analysis and Sensory Evaluation of Ulluco (*Ullucus tuberosus* Loz) Grown in New Zealand. *J. Sci. Food Agric.* **2000**, *80*, 2232–2240. [CrossRef]
5. Campos, D.; Chirinos, R.; Gálvez Ranilla, L.; Pedreschi, R. Bioactive Potential of Andean Fruits, Seeds, and Tubers. In *Advances in Food and Nutrition Research*; Elsevier: Amsterdam, The Netherlands, 2018; Volume 84, pp. 287–343. ISBN 978-0-12-814990-4. [CrossRef]

6. O'Hair, S.K.; Maynard, D.N. VEGETABLES OF TROPICAL CLIMATES | Root Crops of Uplands. In *Encyclopedia of Food Sciences and Nutrition*, 2nd ed.; Caballero, B., Ed.; Academic Press: Oxford, UK, 2003; pp. 5962–5965. Available online: https://www.sciencedirect.com/science/article/pii/B012227055X012438 (accessed on 10 March 2024)ISBN 978-0-12-227055-0.
7. MIDAGRI Perfil Productivo y Competitivo de Los Principales Cultivos Del Sector. Available online: https://app.powerbi.com/view?r=eyJrIjoiYjYwYTk5MDgtM2M0MS00NDMyLTgzNDEtMjNhNjEzYWQyOTNlIiwidCI6IjdmMDg0NjI3LTdmNDAtNDg3OS04OTE3LTk0Yjg2ZmQzNWYzZiJ9 (accessed on 29 February 2024).
8. INEI IV Censo Nacional Agropecuario 2012—Base de Datos REDATAM. Available online: http://censos1.inei.gob.pe/Cenagro/redatam/ (accessed on 21 May 2024).
9. Condori, B.; Mamani, P.; Botello, R.; Patiño, F.; Devaux, A.; Ledent, J.F. Agrophysiological Characterisation and Parametrisation of Andean Tubers: Potato (*Solanum* Sp.), Oca (*Oxalis tuberosa*), Isaño (*Tropaeolum tuberosum*) and Papalisa (*Ullucus tuberosus*). *Eur. J. Agron.* **2008**, *28*, 526–540. [CrossRef]
10. Muñoz, A.M.; Jimenez-Champi, D.; Contreras-López, E.; Fernández-Jerí, Y.; Best, I.; Aguilar, L.; Ramos-Escudero, F. Valorization of Extracts of Andean Roots and Tubers and Its Byproducts: Bioactive Components and Antioxidant Activity in Vitro. *Food Res.* **2023**, *7*, 55–63. [CrossRef]
11. INEI Perú: Consumo Per Cápita de los Principales Alimentos 2008–2009. In *Encuesta Nacional de Presupuestos Familiares (ENAPREF)*; Dirección Técnica de Demografía e Indicadores Sociales-INEI: Lima, Perú, 2012.
12. Abbas, A.; Waseem, M.; Ahmad, R.; Khan, K.A.; Zhao, C.; Zhu, J. Sensitivity Analysis of Greenhouse Gas Emissions at Farm Level: Case Study of Grain and Cash Crops. *Environ. Sci. Pollut. Res.* **2022**, *29*, 82559–82573. [CrossRef]
13. Elahi, E.; Li, G.; Han, X.; Zhu, W.; Liu, Y.; Cheng, A.; Yang, Y. Decoupling Livestock and Poultry Pollution Emissions from Industrial Development: A Step towards Reducing Environmental Emissions. *J. Environ. Manag.* **2024**, *350*, 119654. [CrossRef] [PubMed]
14. IPCC. *Climate Change 2021—The Physical Science Basis: Working Group I Contribution to the Sixth Assessment Report of the Intergovernmental Panel on Climate Change*, 1st ed.; Cambridge University Press: Cambridge, UK, 2023; ISBN 978-1-00-915789-6. [CrossRef]
15. O'Neill, B.C.; Tebaldi, C.; van Vuuren, D.P.; Eyring, V.; Friedlingstein, P.; Hurtt, G.; Knutti, R.; Kriegler, E.; Lamarque, J.-F.; Lowe, J.; et al. The Scenario Model Intercomparison Project (ScenarioMIP) for CMIP6. *Geosci. Model Dev.* **2016**, *9*, 3461–3482. [CrossRef]
16. Ahmadi, S.H.; Reis Ghorra, M.R.; Sepaskhah, A.R. Parameterizing the AquaCrop Model for Potato Growth Modeling in a Semi-Arid Region. *Field Crops Res.* **2022**, *288*, 108680. [CrossRef]
17. Wang, H.; Cheng, M.; Liao, Z.; Guo, J.; Zhang, F.; Fan, J.; Feng, H.; Yang, Q.; Wu, L.; Wang, X. Performance Evaluation of AquaCrop and DSSAT-SUBSTOR-Potato Models in Simulating Potato Growth, Yield and Water Productivity under Various Drip Fertigation Regimes. *Agric. Water Manag.* **2023**, *276*, 108076. [CrossRef]
18. Wellens, J.; Raes, D.; Fereres, E.; Diels, J.; Coppye, C.; Adiele, J.G.; Ezui, K.S.G.; Becerra, L.-A.; Selvaraj, M.G.; Dercon, G.; et al. Calibration and Validation of the FAO AquaCrop Water Productivity Model for Cassava (*Manihot esculenta* Crantz). *Agric. Water Manag.* **2022**, *263*, 107491. [CrossRef]
19. Rankine, D.R.; Cohen, J.E.; Taylor, M.A.; Coy, A.D.; Simpson, L.A.; Stephenson, T.; Lawrence, J.L. Parameterizing the FAO AquaCrop Model for Rainfed and Irrigated Field-Grown Sweet Potato. *Agron. J.* **2015**, *107*, 375–387. [CrossRef]
20. Puma-Cahua, J.; Belizario, G.; Laqui, W.; Alfaro, R.; Huaquisto, E.; Calizaya, E. Evaluating the Yields of the Rainfed Potato Crop under Climate Change Scenarios Using the AquaCrop Model in the Peruvian Altiplano. *Sustainability* **2023**, *16*, 71. [CrossRef]
21. Chumbe, R.; Silva, S.; Garcia, Y. Comparison of the Machine Learning and AquaCrop Models for Quinoa Crops. *Res. Agric. Eng.* **2023**, *69*, 65–75. [CrossRef]
22. Geerts, S.; Raes, D.; Garcia, M.; Taboada, C.; Miranda, R.; Cusicanqui, J.; Mhizha, T.; Vacher, J. Modeling the Potential for Closing Quinoa Yield Gaps under Varying Water Availability in the Bolivian Altiplano. *Agric. Water Manag.* **2009**, *96*, 1652–1658. [CrossRef]
23. Alavi, G.; Diels, J.; Willems, P.; García, M. Simulación de la producción de Quinua en el Altiplano Boliviano con el modelo de Aquacrop con escenarios futuros generados por LARS-WG y QMP. *Rev. Investig. E Innov. Agropecu. Recur. Nat.* **2015**, *2*, 7–13.
24. Bwalya, A. Validation of the Aquacrop Model for Irrigated African Eggplant (*Solanum macrocarpon*) at the Unza Field Station. Ph.D. Thesis, University of Zambia, Lusaka, Zambia, 2012. Available online: https://library.adhl.africa/handle/123456789/12619 (accessed on 10 March 2024).
25. Cobeña, O.; Pamela, C. Calibración, validación y utilización del modelo AquaCrop para el cultivo de la chufa (*Cyperus esculentus* L. var. sativus Boeck.) en Valencia. Master's Thesis, Universitat Politècnica de Valencia, Valencia, Spain, 2020. Available online: https://riunet.upv.es/handle/10251/134097 (accessed on 10 March 2024).
26. Mabhaudhi, T.; Modi, A.T.; Beletse, Y.G. Parameterization and Evaluation of the FAO-AquaCrop Model for a South African Taro (*Colocasia esculenta* L. Schott) Landrace. *Agric. For. Meteorol.* **2014**, *192*, 132–139. [CrossRef]
27. Sharma, V.; Singh, P.K. Performance of AquaCrop Model for Predicting Yield and Biomass of Okra (*Abelmoschus esculentus*) Crop. *Indian J. Agric. Sci.* **2023**, *93*, 899–905. [CrossRef]
28. Walker, S.; Bello, Z.A.; Mabhaudhi, T.; Modi, A.T.; Beletse, Y.G.; Zuma-Netshiukhwi, G. Calibration of AquaCrop Model to Predict Water Requirements of Traditional African Vegetables. *Acta Hortic.* **2013**, *1007*, 943–949. [CrossRef]

29. Steduto, P.C.; Hsiao, T.; Fereres, E.; Raes, D. Land and Water Division. In *Crop Yield Response to Water*; FAO Irrigation and Drainage Paper; FAO: Rome, Italy, 2012; ISBN 978-92-5-107274-5. Available online: https://www.fao.org/documents/card/en/c/c355da16-217c-555b-acbc-505d87bade00 (accessed on 10 March 2024).
30. Vanuytrecht, E.; Raes, D.; Steduto, P.; Hsiao, T.C.; Fereres, E.; Heng, L.K.; Garcia Vila, M.; Mejias Moreno, P. AquaCrop: FAO's Crop Water Productivity and Yield Response Model. *Environ. Model. Softw.* **2014**, *62*, 351–360. [CrossRef]
31. Dewedar, O.; Plauborg, F.; El-Shafie, A.; Marwa, A. Response of Potato Biomass and Tuber Yield under Future Climate Change Scenarios in Egypt. *J. Water Land Dev.* **2021**, *49*, 139–150. [CrossRef]
32. Yaghoobzadeh, M.; Azarmi Atajan, F.; Arabi Ayask, M.; Ghadirian, A.H. Investigating the Effect of Drip and Furrow Irrigation Methods on the Simulation of Sugar Beet Yield by Using the AquaCrop Model. *J. Water Res. Agric.* **2023**, *37*, 323–335. [CrossRef]
33. FAO Limitations | AquaCrop | Food and Agriculture Organization of the United Nations. Available online: https://www.fao.org/aquacrop/overview/limitations/en/ (accessed on 12 May 2024).
34. IPCC. *Climate Change 2022—Impacts, Adaptation and Vulnerability: Working Group II Contribution to the Sixth Assessment Report of the Intergovernmental Panel on Climate Change*, 1st ed.; Cambridge University Press: Cambridge, UK, 2023; ISBN 978-1-00-932584-4.
35. Tito, R.; Vasconcelos, H.L.; Feeley, K.J. Global Climate Change Increases Risk of Crop Yield Losses and Food Insecurity in the Tropical Andes. *Glob. Chang. Biol.* **2018**, *24*, e592–e602. [CrossRef]
36. Yzarra, W.; Trebejo, I.; Kanamura, H.; Fujisawa, M.; Guerrero, J.; Bello, D.; Villanueva, J.; Soriano, V. *Componente 1: Evaluación de Los Impactos del Cambio Climático Sobre el Rendimiento de Los Cultivos en el Perú*; Servicio Nacional de Meteorologia e Hidrologia: Lima, Peru, 2015.
37. Tarmizi, A.H.A. Climate Change and Its Impact on Rainfall. *Int. J. Integr. Eng.* **2019**, *11*, 170–177.
38. Sanabria, J.; Calanca, P.; Alarcón, C.; Canchari, G. Potential Impacts of Early Twenty-First Century Changes in Temperature and Precipitation on Rainfed Annual Crops in the Central Andes of Peru. *Reg. Environ. Chang.* **2014**, *14*, 1533–1548. [CrossRef]
39. Bisbis, M.B.; Gruda, N.; Blanke, M. Potential Impacts of Climate Change on Vegetable Production and Product Quality—A Review. *J. Clean. Prod.* **2018**, *170*, 1602–1620. [CrossRef]
40. Kalliola, R.; Jokela, P.; Pietila, L.; Rousi, A.; Salo, J.; Yli-Rekola, M. Influencia del fotoperíodo en el crecimiento y formación de tubérculos de ulluco (*Ullucus tuberosus*, Basellaceae), Oca (*Oxalis tuberosa*, Oxalidaceae) y Añu (*Tropaeolum tuberosum*, Tropaeolaceae). In *Turrialba*; IICA: San José, Costa Rica, 1990; Available online: https://repositorio.catie.ac.cr/handle/11554/10460 (accessed on 10 March 2024).
41. Markarov, A.M. Causes of Flowering of Long-Day Potato Species under Short-Day and Cold-Night Conditions. *Russ. J. Plant Physiol.* **2002**, *49*, 465–469. [CrossRef]
42. Martin, R.J.; Scheffer, J.J.C.; Deo, B.; Halloy, S.R.P. Effect of Planting Date on Ulluco Yield. *Acta Hortic.* **2005**, *670*, 181–187. [CrossRef]
43. Scheffer, J.J.C.; Douglas, J.A.; Martin, R.J.; Halloy, S.R.P.; Deo, B.; Triggs, C.M. Agronomic Requirements of Ulluco (*Ullucus Tuberosus*)—A South American Tuber. *Agronomy* **2002**, *32*, 41–47.
44. Acurio, L.; Salazar, D.; Castillo, B.; Santiana, C.; Martínez-Monzó, J.; Igual, M. Characterization of Second-Generation Snacks Manufactured from Andean Tubers and Tuberous Root Flours. *Foods* **2024**, *13*, 51. [CrossRef] [PubMed]
45. Mosquera, N.; Cejudo-Bastante, M.J.; Heredia, F.J.; Hurtado, N. Identification of New Betalains in Separated Betacyanin and Betaxanthin Fractions from Ulluco (*Ullucus Tuberosus* Caldas) by HPLC-DAD-ESI-MS. *Plant Foods Hum. Nutr. Dordr. Neth.* **2020**, *75*, 434–440. [CrossRef] [PubMed]
46. Velasquez Barreto, F.F.; Bello-Pérez, L.A. Chemical, Structural, Technological Properties and Applications of Andean Tuber Starches: A Review. *Food Rev. Int.* **2023**, *39*, 1293–1308. [CrossRef]
47. Keleman Saxena, A.; Cadima Fuentes, X.; Gonzales Herbas, R.; Humphries, D.L. Indigenous Food Systems and Climate Change: Impacts of Climatic Shifts on the Production and Processing of Native and Traditional Crops in the Bolivian Andes. *Front. Public Health* **2016**, *4*, 175055. [CrossRef] [PubMed]
48. Ponce, N.L.C.; Martínez, M.E.P. Tubérculos andinos y conocimiento agrícola local en comunidades rurales de Ecuador y Colombia. *Cuad. Desarro. Rural* **2014**, *11*, 149–166. [CrossRef]
49. López, G.; Yupanqui, A.T.; Fierro, R.E. Fenología y Agronomía del Cultivo. In *El Cultivo del Ulluco en la Sierra Central del Perú*; López, G., Hermann, M., Eds.; Conservación y uso de la biodiversidad de raíces y tubérculos andinos: Una década de investigación para el desarrollo (1993–2003); Centro Internacional de la Papa (CIP): Lima, Peru, 2004.
50. SENAMHI. SENAMHI—Descarga de Datos. Available online: https://www.senamhi.gob.pe/site/descarga-datos/ (accessed on 29 February 2024).
51. López, G. Tubérculos-Semilla. In *El Cultivo del Ulluco en la Sierra Central del Perú*; López, G., Hermann, M., Eds.; Conservación y uso de la biodiversidad de raíces y tubérculos andinos: Una década de investigación para el desarrollo (1993–2003); Centro Internacional de la Papa (CIP): Lima, Peru, 2004.
52. *ISO 11272:2017*; Soil Quality—Determination of Dry Bulk Density. ISO (International Organization for Standardization): Geneva, Switzerland, 2017. Available online: https://www.iso.org/standard/68255.html (accessed on 25 March 2024).
53. *NOM-021-RECNAT-2000*; Norma Oficial Mexicana Que Establece Las Especificaciones de Fertilidad, Salinidad y Clasificación de Suelos. Estudios, Muestreo y Análisis. 2002. Available online: https://faolex.fao.org/docs/pdf/mex50674.pdf (accessed on 10 March 2024).

54. USEPA. *METHOD 9045D. SOIL AND WASTE pH 2004*; USEPA: Washington, DC, USA, 2004. Available online: https://www.epa.gov/sites/default/files/2015-12/documents/9045d.pdf (accessed on 25 March 2024).
55. *ISO 11265:1994*; Soil Quality—Determination of the Specific Electrical Conductivity. ISO (International Organization for Standardization): Geneva, Switzerland, 1994. Available online: https://www.iso.org/standard/19243.html (accessed on 25 March 2024).
56. *ISO 11461:2001*; Soil Quality—Determination of Soil Water Content as a Volume Fraction Using Coring Sleeves—Gravimetric Method. ISO (International Organization for Standardization): Geneva, Switzerland, 2001. Available online: https://www.iso.org/standard/33031.html (accessed on 25 March 2024).
57. Horikoshi, M.; Tang, Y.; Dickey, A.; Grenié, M.; Thompson, R.; Selzer, L.; Strbenac, D.; Voronin, K.; Pulatov, D. Ggfortify: Data Visualization Tools for Statistical Analysis Results 2024. Available online: https://cran.r-project.org/web/packages/ggfortify/index.html (accessed on 26 January 2024).
58. Mendiburu, F. de Agricolae: Statistical Procedures for Agricultural Research, version 1.3-7. 2023. Available online: https://cran.r-project.org/web/packages/agricolae/index.html (accessed on 26 January 2024).
59. Paulhus, J.L.H.; Kohler, M.A. Interpolation of Missing Precipitation Records. *Mon. Weather Rev.* **1952**, *80*, 129–133. [CrossRef]
60. Guijarro, J.A. Climatol: Climate Tools (Series Homogenization and Derived Products), version 4.1.0. 2023. Available online: https://cran.r-project.org/web/packages/climatol/index.html (accessed on 26 January 2024).
61. Almazroui, M.; Ashfaq, M.; Islam, M.N.; Rashid, I.U.; Kamil, S.; Abid, M.A.; O'Brien, E.; Ismail, M.; Reboita, M.S.; Sörensson, A.A.; et al. Assessment of CMIP6 Performance and Projected Temperature and Precipitation Changes Over South America. *Earth Syst. Environ.* **2021**, *5*, 155–183. [CrossRef]
62. Fernandez-Palomino, C.A.; Hattermann, F.F.; Krysanova, V.; Vega-Jácome, F.; Menz, C.; Gleixner, S.; Bronstert, A. High-Resolution Climate Projection Dataset Based on CMIP6 for Peru and Ecuador: BASD-CMIP6-PE. *Sci. Data* **2024**, *11*, 34. [CrossRef] [PubMed]
63. Hijmans, R.J.; Bivand, R.; Pebesma, E.; Sumner, M.D. Terra: Spatial Data Analysis, version 1.7-71. 2023. Available online: https://cran.r-project.org/web/packages/terra/index.html (accessed on 26 January 2024).
64. Gudmundsson, L. Qmap: Statistical Transformations for Post-Processing Climate Model Output, version 1.0-4. 2016. Available online: https://cran.r-project.org/web/packages/qmap/index.html (accessed on 26 January 2024).
65. Boucher, O.; Denvil, S.; Levavasseur, G.; Cozic, A.; Caubel, A.; Foujols, M.-A.; Meurdesoif, Y.; Cadule, P.; Devilliers, M.; Ghattas, J.; et al. IPSL IPSL-CM6A-LR Model Output Prepared for CMIP6 CMIP Historical. 2018. [CrossRef]
66. Voldoire, A. *CMIP6 Simulations of the CNRM-CERFACS Based on CNRM-CM6-1 Model for CMIP Experiment Historical*; Earth System Grid Federation: Greenbelt, MD, USA, 2018; Available online: http://cera-www.dkrz.de/WDCC/meta/CMIP6/CMIP6.CMIP.CNRM-CERFACS.CNRM-CM6-1.historical (accessed on 28 February 2024).
67. Seferian, R. *CNRM-CERFACS CNRM-ESM2-1 Model Output Prepared for CMIP6 CMIP Historical*; Earth System Grid Federation: Greenbelt, MD, USA, 2018; Available online: http://cera-www.dkrz.de/WDCC/meta/CMIP6/CMIP6.CMIP.CNRM-CERFACS.CNRM-ESM2-1.historical (accessed on 28 February 2024).
68. Tatebe, H.; Watanabe, M. *MIROC MIROC6 Model Output Prepared for CMIP6 CMIP Historical*; Earth System Grid Federation: Greenbelt, MD, USA, 2018; Available online: http://cera-www.dkrz.de/WDCC/meta/CMIP6/CMIP6.CMIP.MIROC.MIROC6.historical (accessed on 28 February 2024).
69. Yukimoto, S.; Koshiro, T.; Kawai, H.; Oshima, N.; Yoshida, K.; Urakawa, S.; Tsujino, H.; Deushi, M.; Tanaka, T.; Hosaka, M.; et al. *MRI MRI-ESM2.0 Model Output Prepared for CMIP6 CMIP Historical*; WCRP: Geneva, Switzerland, 2019; Available online: http://cera-www.dkrz.de/WDCC/meta/CMIP6/CMIP6.CMIP.MRI.MRI-ESM2-0.historical (accessed on 28 February 2024).
70. Jungclaus, J.; Bittner, M.; Wieners, K.-H.; Wachsmann, F.; Schupfner, M.; Legutke, S.; Giorgetta, M.; Reick, C.; Gayler, V.; Haak, H.; et al. *MPI-M MPI-ESM1.2-HR Model Output Prepared for CMIP6 CMIP Historical*; WCRP: Geneva, Switzerland, 2019.
71. EC-Earth Consortium (EC-Earth). *EC-Earth-Consortium EC-Earth3 Model Output Prepared for CMIP6 CMIP Historical*; Earth System Grid Federation: Greenbelt, MD, USA, 2019. [CrossRef]
72. EFSA Panel on Plant Health (PLH); Bragard, C.; Dehnen-Schmutz, K.; Di Serio, F.; Gonthier, P.; Jacques, M.; Jaques Miret, J.A.; Justesen, A.F.; MacLeod, A.; Magnusson, C.S.; et al. Commodity Risk Assessment of *Ullucus Tuberosus* Tubers from Peru. *EFSA J.* **2021**, *19*, e06428. [CrossRef] [PubMed]
73. EC-Earth Consortium (EC-Earth). *EC-Earth-Consortium EC-Earth3 model output prepared for CMIP6 ScenarioMIP ssp126*; Earth System Grid Federation: Greenbelt, MD, USA, 2019. [CrossRef]
74. EC-Earth Consortium (EC-Earth). *EC-Earth-Consortium EC-Earth3 model output prepared for CMIP6 ScenarioMIP ssp370*; Earth System Grid Federation: Greenbelt, MD, USA, 2019. [CrossRef]
75. EC-Earth Consortium (EC-Earth). *EC-Earth-Consortium EC-Earth3 model output prepared for CMIP6 ScenarioMIP ssp585*; Earth System Grid Federation: Greenbelt, MD, USA, 2019. [CrossRef]
76. Castro, A.; Davila, C.; Laura, W.; Cubas, F.; Avalos, G.; López-Ocaña, C.; Villena, D.; Valdez, M.; Urbiola, J.; Trebejo, I.; et al. CLIMAS DEL PERÚ—Mapa de Clasificación Climática Nacional, 1st ed. 2021. Available online: https://www.senamhi.gob.pe/load/file/01404SENA-4.pdf (accessed on 22 May 2024).
77. Wongchuig, S.C.; Mello, C.R.; Chou, S.C. Projections of the Impacts of Climate Change on the Water Deficit and on the Precipitation Erosive Indexes in Mantaro River Basin, Peru. *J. Mt. Sci.* **2018**, *15*, 264–279. [CrossRef]

78. Arana Ruedas, D.P.R.; Soto Guerra, L.; Popli, K.; Madaki, S.G.; Arana Ruedas, D.P.R.; Soto Guerra, L.; Popli, K.; Madaki, S.G. Evaluación Espacio-Temporal de Sequías Usando El Índice Estandarizado de Precipitación y Evapotranspiración (SPEI) En El Valle Del Mantaro, Perú. *Rev. Investig. Altoandinas* **2023**, *25*, 159–170. [CrossRef]
79. Saavedra, M.; Junquas, C.; Espinoza, J.-C.; Silva, Y. Impacts of Topography and Land Use Changes on the Air Surface Temperature and Precipitation over the Central Peruvian Andes. *Atmos. Res.* **2020**, *234*, 104711. [CrossRef]
80. Yin, Y.; Deng, H.; Wu, S. Spatial-Temporal Variations in the Thermal Growing Degree-Days and Season under Climate Warming in China during 1960–2011. *Int. J. Biometeorol.* **2019**, *63*, 649–658. [CrossRef]
81. Wahid, A.; Gelani, S.; Ashraf, M.; Foolad, M.R. Heat Tolerance in Plants: An Overview. *Environ. Exp. Bot.* **2007**, *61*, 199–223. [CrossRef]
82. Sage, T.L.; Bagha, S.; Lundsgaard-Nielsen, V.; Branch, H.A.; Sultmanis, S.; Sage, R.F. The Effect of High Temperature Stress on Male and Female Reproduction in Plants. *Field Crops Res.* **2015**, *182*, 30–42. [CrossRef]
83. Chaves-Barrantes, N.F.; Gutiérrez-Soto, M.V. Respuestas al estrés por calor en los cultivos. I. aspectos moleculares, bioquímicos y fisiológicos. *Agron. Mesoam.* **2017**, *28*, 237–253. [CrossRef]
84. Sita, K.; Sehgal, A.; HanumanthaRao, B.; Nair, R.M.; Vara Prasad, P.V.; Kumar, S.; Gaur, P.M.; Farooq, M.; Siddique, K.H.M.; Varshney, R.K.; et al. Food Legumes and Rising Temperatures: Effects, Adaptive Functional Mechanisms Specific to Reproductive Growth Stage and Strategies to Improve Heat Tolerance. *Front. Plant Sci.* **2017**, *8*, 298433. [CrossRef] [PubMed]
85. Nieto-Cabrera, C.; Francis, C.; Caicedo, C.; Gutierrez, P.F.; Rivera, M. Response of Four Andean Crops to Rotation and Fertilization. *Mt. Res. Dev.* **1997**, *17*, 273. [CrossRef]
86. Meldrum, G.; Mijatović, D.; Rojas, W.; Flores, J.; Pinto, M.; Mamani, G.; Condori, E.; Hilaquita, D.; Gruberg, H.; Padulosi, S. Climate Change and Crop Diversity: Farmers' Perceptions and Adaptation on the Bolivian Altiplano. *Environ. Dev. Sustain.* **2018**, *20*, 703–730. [CrossRef]
87. FAO. *Climate Change and Food Security: Risks and Responses*; FAO: Rome, Italy, 2015; ISBN 978-92-5-108998-9. Available online: https://openknowledge.fao.org/server/api/core/bitstreams/a4fd8ac5-4582-4a66-91b0-55abf642a400/content (accessed on 22 May 2024).
88. MINAM. *Plan Nacional de Adaptación al Cambio Climático Del Perú: Un Insumo Para La Actualización de La Estrategia Nacional Ante El Cambio Climático—Resumen Ejecutivo*, 1st ed.; Ministerio del Ambiente (MINAM): Lima, Peru, 2022. Available online: https://cdn.www.gob.pe/uploads/document/file/2827898/220214_Resumen%20Ejecutivo%20del%20Plan%20Nacional%20de%20Adaptaci%C3%B3n_compressed.pdf.pdf?v=1664915422 (accessed on 22 May 2024).
89. Calderón, R.R. *Estadisticas de las Tecnologías de Información y Comunicación en los Hogares*; Instituto Nacional de Estadística e Informática (INEI): Lima, Peru, 2021. Available online: https://cdn.www.gob.pe/uploads/document/file/3093592/Las%20Tecnolog%C3%ADas%20de%20Informaci%C3%B3n%20y%20Comunicaci%C3%B3n%20en%20los%20Hogares:%20Abr-May-Jun%202021.pdf?v=1652377629 (accessed on 5 June 2024).
90. SENAMHI. Pronóstico de Riego Agroclimático Nacional. Available online: https://www.senamhi.gob.pe/?&p=impacto-en-la-agricultura (accessed on 5 June 2024).